GEOLOGY | THE GEOLOGICAL SOCIETY OF AMERICA®

https://doi.org/10.1130/G46861.1

Manuscript received 10 August 2019
Revised manuscript received 17 October 2019
Manuscript accepted 29 October 2019

Published online XX Month 2019

Sea level, carbonate mineralogy, and early diagenesis controlled $\delta^{13}C$ records in Upper Ordovician carbonates

David S. Jones[1], R. William Brothers[1], Anne-Sofie Crüger Ahm[2], Nicholas Slater[2], John A. Higgins[2] and David A. Fike[3]
[1]Geology Department, Amherst College, 11 Barrett Hill Road, Amherst, Massachusetts 01002, USA
[2]Department of Geosciences, Princeton University, Guyot Hall, Princeton, New Jersey 08544, USA
[3]Department of Earth & Planetary Sciences, Washington University in St. Louis, 1 Brookings Drive, St. Louis, Missouri 63130, USA

ABSTRACT

Stratigraphic variability in the geochemistry of sedimentary rocks provides critical data for interpreting paleoenvironmental change throughout Earth history. However, the vast majority of pre-Jurassic geochemical records derive from shallow-water carbonate platforms that may not reflect global ocean chemistry. Here, we used calcium isotope ratios ($\delta^{44}Ca$) in conjunction with minor-element geochemistry (Sr/Ca) and field observations to explore the links among sea-level change, carbonate mineralogy, and marine diagenesis and the expression of a globally documented interval of elevated carbon isotope ratios ($\delta^{13}C$; Hirnantian isotopic carbon excursion [HICE]) associated with glaciation in Upper Ordovician shallow-water carbonate strata from Anticosti Island, Canada, and the Great Basin, Nevada and Utah, USA. The HICE on Anticosti is preserved in limestones with low $\delta^{44}Ca$ and high Sr/Ca, consistent with aragonite as a major component of primary mineralogy. Great Basin strata are characterized by lateral gradients in $\delta^{44}Ca$ and $\delta^{13}C$ that reflect variations in the extent of early marine diagenesis across the platform. In deep-ramp settings, deposition during synglacial sea-level lowstand and subsequent postglacial flooding increased the preservation of an aragonitic signature with elevated $\delta^{13}C$ produced in shallow-water environments. In contrast, on the mid- and inner ramp, extensive early marine diagenesis under seawater-buffered conditions muted the magnitude of the shift in $\delta^{13}C$. The processes documented here provide an alternative explanation for variability in a range of geochemical proxies preserved in shallow-water carbonates at other times in Earth history, and challenge the notion that these proxies necessarily record changes in the global ocean.

INTRODUCTION

Ancient shallow-water carbonate strata provide important archives of the evolution of Earth's climate and environments. In particular, the carbon isotopic composition ($^{13}C/^{12}C$) of ancient shallow-water carbonate sediments has been widely applied as both a chronostratigraphic tool (Saltzman and Thomas, 2012) and an indicator of the partitioning of global carbon fluxes between carbonate and organic reservoirs, linking the global geochemical cycles of carbon and oxygen (Kump and Arthur, 1999; Saltzman et al., 2011). However, this interpretation of the carbon isotopic composition of shallow-water carbonates has been questioned by studies of modern analogues (Swart and Eberli, 2005; Swart, 2008; Higgins et al., 2018), where local processes, early diagenetic alteration, and changes in $\delta^{13}C$ of carbonate minerals conspire to decouple the chemistry of shallow-water carbonate sediments from the global ocean.

Hirnantian $\delta^{13}C$ and Sea Level

Upper Ordovician (Hirnantian) strata around the globe contain an interval of elevated $\delta^{13}C$, referred to as the Hirnantian isotopic carbon excursion (HICE). The HICE is associated with sea-level fall during the Hirnantian glaciation, which lasted less than 1.3 m.y. and has a geographically variable magnitude, ranging from ~+2‰ to ~+7‰ (Melchin et al., 2013, and references therein). Geochemical anomalies in $\delta^{15}N$, $\delta^{34}S$, $^{87}Sr/^{86}Sr$, $\delta^{26}Mg$, and $\delta^{7}Li$ (LaPorte et al., 2009; Zhang et al., 2009; Hu et al., 2017; Kimmig and Holmden, 2017; Pogge von Strandmann et al., 2017) are also found in Hirnantian strata. The origin of the HICE has been attributed to increased global organic carbon burial (Brenchley et al., 1994); synglacial changes in $\delta^{13}C$ of the riverine weathering flux (Kump et al., 1999); and/or local carbon cycling in shallow basins partially isolated from the global ocean (Melchin and Holmden, 2006). However, these models can require unrealistic changes to carbon burial and/or weathering fluxes, or they predict cross-platform $\delta^{13}C$ gradients ($\delta^{13}C$ increasing with greater proximity to the coast) that contradict the variability observed in some basins.

Here, we developed a new hypothesis that explains the HICE as a record of shallow-water aragonite $\delta^{13}C$ that evolved during sea-level change and was variably altered during early marine diagenesis. We used measurements of $\delta^{44}Ca$, $\delta^{13}C$, and Sr/Ca to identify the primary mineralogy and early diagenetic history of carbonates deposited across the Hirnantian interval. We propose a mechanism that links the observed magnitude of the HICE to glacioeustasy, depositional environment, and early diagenesis, and we discuss the implications for understanding the links between elevated $\delta^{13}C$ and global environmental change in the geologic record.

Diagenetic Framework for Shallow-Water Marine Carbonate Sediments

The pairing of calcium isotopes ($\delta^{44}Ca$) and trace-element ratios (Sr/Ca and Mg/Ca) has emerged as a promising tool to identify both primary mineralogy and the style of early diagenetic alteration of marine carbonate sediments (Fantle and DePaolo, 2007; Fantle and Higgins, 2014; Higgins et al., 2018). In particular, crossplots of $\delta^{44}Ca$ and Sr/Ca in carbonates of all geologic ages exhibit covariation that can be quantitatively related to the style of early marine diagenesis. The covariation arises for three reasons. First, early diagenetic carbonate minerals are characterized by low Sr/Ca partition coefficients (Brand and Veizer, 1980) and small Ca isotope fractionation factors (Fantle and DePaolo, 2007; Jacobson and Holmden, 2008; Tang et al., 2008) compared to primary marine carbonate minerals (although Baker et al. [1982] showed that deep-sea pelagic calcite can maintain high

CITATION: Jones, D.S., et al., 2020, Sea level, carbonate mineralogy, and early diagenesis controlled 13C records in Upper Ordovician carbonates: Geology, v. 48, p. XXX–XXX, https://doi.org/10.1130/G46861.1

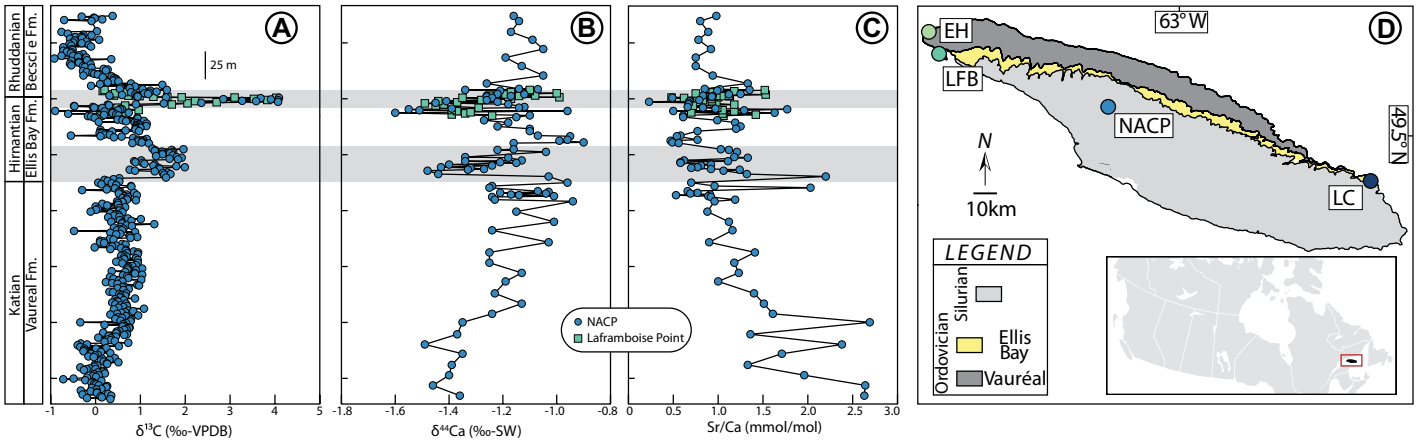

Figure 1. Stratigraphic plots of geochemical data from Anticosti Island, Canada: New Associated Consolidated Paper (NACP) drill core and Laframboise Point outcrop limestones. (A) $\delta^{13}C$. (B) $\delta^{44}Ca$. (C) Sr/Ca. Laframboise Point carbon isotope data are from Jones et al. (2011). Horizontal gray bands indicate lower and upper Hirnantian isotopic carbon excursion (HICE) carbon isotope anomalies. (D) Simplified geologic map of Anticosti Island, after Desrochers et al. (2010). EH—English Head, LFB—Laframboise Point, LC—Lousy Cove, Fm.—Formation, SW—seawater, VPDB—Vienna Peedee belemnite.

Sr/Ca during marine diagenesis). Second, $\delta^{44}Ca$ and Sr/Ca depend on primary mineralogy, with aragonite precipitation fractionating Ca isotopes to a greater extent (Gussone et al., 2005) and incorporating more Sr (Veizer, 1983) than calcite. Third, early marine diagenesis in shallow-water carbonate sediments can occur under both fluid- and sediment-buffered conditions, depending on the extent to which pore-fluid exchange with seawater occurs through advection or diffusion (Banner and Hanson, 1990; Fantle and DePaolo, 2007; Fantle and Higgins, 2014; Higgins et al., 2018). Together, these properties of primary and diagenetic carbonate minerals and shallow-water sedimentary systems lead to a characteristic relationship between bulk $\delta^{44}Ca$ and Sr/Ca and provide a means with which to characterize the effects of mineralogy and early marine diagenesis on the geochemistry of shallow-water carbonate sediments (Ahm et al., 2018; Higgins et al., 2018).

METHODS

We generated $\delta^{44}Ca$ ($\delta^{44/40}Ca$) and Sr/Ca data from 328 samples from two Upper Ordovician carbonate ramps. Limestone samples from the Vaureal and Ellis Bay Formations (Anticosti Island, Canada; Fig. 1D) were selected from those reported by Jones et al. (2011). Additional Anticosti material was sampled from the New Associated Consolidated Paper (NACP) drill core (49°37.337′N, 63°26.292′W; Desrochers et al., 2010; McLaughlin et al., 2016). Samples of the Ely Springs Dolostone (Great Basin, Nevada and Utah, USA; Fig. 2D) were selected from those reported by Jones et al. (2016) along a depth transect from shallow- to mid-ramp settings (Carpenter et al., 1986). Data from a deep-ramp section (Holmden et al., 2012) completed the Great Basin transect.

Samples were analyzed for cation ratios and calcium stable isotopic composition at Princeton University (New Jersey, USA) following the methods of Higgins et al. (2018). Ca isotope measurements are reported as the relative abundance of ^{44}Ca to ^{40}Ca using standard delta notation, normalized to the isotopic composition of modern seawater. The external reproducibility for SRM915b calcium carbonate standard was $-1.16‰ \pm 0.19‰$ (2σ, $N = 38$), and reproducibility for an internal aragonite standard was $-1.47‰ \pm 0.15‰$ (2σ, $N = 12$). New $\delta^{13}C$ data were generated for the NACP core following the methods of Jones et al. (2011); all other $\delta^{13}C$ data came from Jones et al. (2011, 2016).

RESULTS

The Anticosti Island and Great Basin data varied stratigraphically and geographically in $\delta^{13}C$, $\delta^{44}Ca$, and Sr/Ca (Figs. 1 and 2; Fig. DR1 in the GSA Data Repository[1]). Ca isotope values for limestones were between –0.9‰ and –1.7‰; dolostone values were between –0.5‰ and –1.5‰. Great Basin dolostones showed low Sr/Ca (0.06–0.23 mmol/mol), whereas Anticosti limestones had higher Sr/Ca that spanned a wider range (0.22–2.69 mmol/mol). Cross-plots of $\delta^{44}Ca$ and Sr/Ca revealed covariation similar to that observed for Neogene carbonates from the Bahamas (Figs. 3A and 3C). Cross-plots of $\delta^{44}Ca$ and $\delta^{13}C$ showed a slight negative correlation for Ordovician and Neogene samples (Figs. 3B and 3D); Ordovician samples with elevated $\delta^{13}C$, including the HICE, were characterized by $\delta^{44}Ca < -1.0‰$ and elevated Sr/Ca.

DISCUSSION

Measured $\delta^{44}Ca$ and Sr/Ca values of limestones and dolostones from Anticosti Island and the Great Basin spanning the HICE carry a geochemical fingerprint of mineralogy, early marine diagenesis, and dolomitization that is indistinguishable from Neogene platform top and margin strata from the Bahamas.

First, the range in $\delta^{44}Ca$ and Sr/Ca values in the Ordovician data set spans the range of values observed for the Neogene Bahamas (Fig. 3; Fig. DR2), indicating that these sediments experienced a scope of early diagenetic conditions from sediment-buffered (geochemical records set by the chemistry of the primary sediment: low $\delta^{44}Ca$; high Sr/Ca) to fluid-buffered (geochemical records modified by the seawater-like chemistry of fluid flushed through pore space: high $\delta^{44}Ca$; low Sr/Ca; Higgins et al., 2018; Ahm et al., 2018).

Second, strata containing the HICE in Monitor Range, Nevada, and in the NACP core (Figs. 1 and 2) are distinguished by $\delta^{44}Ca$ and Sr/Ca values characteristic of a primary mineralogy dominated by aragonite, indicating that the HICE records a change in the $\delta^{13}C$ of shallow-water aragonite and the dissolved inorganic carbon (DIC) in these environments. The $\delta^{13}C$ of shallow-water DIC likely evolved during Hirnantian sea-level change, as Anticosti samples with high Sr/Ca and low $\delta^{44}Ca$ span a range of $\delta^{13}C$ from ~1‰ to ~4‰. This change is similar to the ~2‰ increase in the $\delta^{13}C$ of shallow-water aragonite in the Bahamas toward the Holocene (Swart and Eberli, 2005; Swart, 2008), albeit on a different time scale. As this Neogene increase is demonstrably decoupled from the $\delta^{13}C$ of the global ocean, we suspect the same is true for the HICE—it reflects a change

[1]GSA Data Repository item 2020055, detailed geologic setting, supplemental discussion of calcium isotope data, location coordinates, Figure DR1 (additional geochemical data), Figure DR2 (histogram of Ordovician and Neogene calcium isotope data), and Table DR1 (geochemical data), is available online at http://www.geosociety.org/datarepository/2020/, or on request from editing@geosociety.org. The Data are archived at EarthChem, at https://doi.org/10.1594/IEDA/111428.

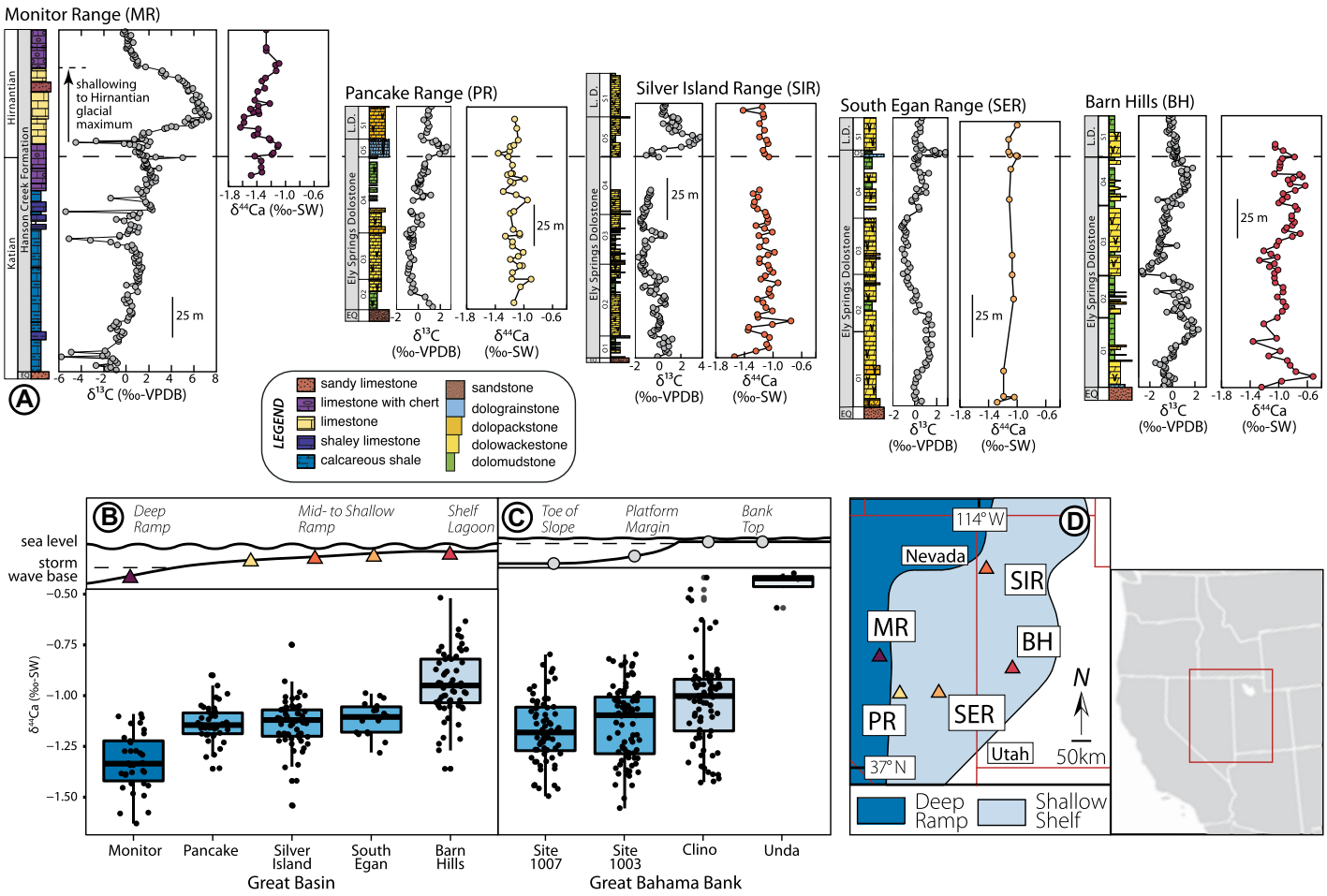

Figure 2. (A) Stratigraphic plots of geochemical data from Great Basin (Nevada and Utah, USA) outcrops: $\delta^{13}C$ and $\delta^{44}Ca$. Datum (horizontal dashed line) is top of Katian-aged strata at each section. Carbon isotope data are from Jones et al. (2016); Monitor Range (Nevada) calcium isotope data are from Holmden et al. (2012). O1–O5 and S1 refer to stratigraphic sequences identified by Harris and Sheehan (1997), with O1–O4 in the Katian and O5 representing the Hirnantian. L.D.—Laketown Dolomite, EQ—Eureka Quartzite; SW—seawater, VPDB—Vienna Peedee belemnite. (B) Ordovician and (C) Neogene calcium isotope gradients across carbonate platforms (not to scale). Both settings demonstrate pattern of increasing $\delta^{44}Ca$ toward basin margin, interpreted to represent increasing magnitude of seawater fluid-buffered diagenesis. Bahamas data are from Higgins et al. (2018). (D) Simplified paleogeographic map of Great Basin carbonate ramp showing locations of shallow shelf and deep ramp, after Harris and Sheehan (1997).

in the $\delta^{13}C$ of shallow-water DIC and associated aragonite but not a change in the $\delta^{13}C$ of DIC in the global ocean.

Finally, the Great Basin exhibits a distinct geographic pattern in $\delta^{44}Ca$ across the ramp that bears a strong resemblance to observations in the Bahamas (Figs. 2B and 2C). The inner-ramp section is characterized by the highest $\delta^{44}Ca$; here, the HICE is missing due to nondeposition or erosion. Three mid-ramp sections preserve a modest HICE and intermediate $\delta^{44}Ca$, whereas deep-ramp limestones at Monitor Range have the lowest $\delta^{44}Ca$ and the largest-magnitude HICE (Holmden et al., 2012). We interpret this cross-platform geochemical gradient to be a consequence of spatially variable pore-fluid flushing by seawater. The interpretation that flushing was highest in the landward direction is consistent with models of fluid convection on the Great Bahama Bank, in which pore-fluid velocity is typically greatest on the shallow bank-top relative to the slope (Caspard et al., 2004). Glacial-interglacial sea-level changes may have enhanced fluid flow and promoted dolomitization in both the Bahamas (Swart and Melim, 2000) and the Ordovician strata considered here. While cross-platform variations in submarine groundwater discharge and carbonate saturation state can produce geographically variable $\delta^{44}Ca$ (Holmden et al., 2012; Shao et al., 2018), our geochemical and geological observations suggest that these factors were negligible in the Great Basin (see the Data Repository).

Taken together, the Ca and C isotope records from Anticosti Island and the Great Basin provide a new framework with which to interpret the origin, preservation, and diagenetic alteration of positive $\delta^{13}C$ values associated with icehouse climates. In this model, platform carbonate sediments are dominated by aragonite. While the Ordovician ocean is commonly considered to have been a "calcite sea" (Hardie, 1996), low-latitude shallow platforms were warm even during the Hirnantian (Finnegan et al., 2011) and would have readily precipitated aragonite (Balthasar and Cusack, 2015; see also the Data Repository). Schematically, we envision the following scenario (Fig. 4): Before glaciation, aragonite $\delta^{13}C$ hovered around 0‰, with increases in shallower environments. Rapid flushing of seawater shifted the $\delta^{13}C$ signal toward seawater values (Fig. 4A). Sea-level fall associated with the Hirnantian glaciation moved shallow-water environments to more distal settings that had previously existed as deeper-ramp environments (Fig. 4B). Changes in the carbon cycle on the platform during the sea-level lowstand resulted in elevated aragonite $\delta^{13}C$ on the ramp (Fig. 4B). The mechanism for increased $\delta^{13}C$ in platform waters remains enigmatic (as it is for the ~2‰ increase in the Bahamas over the Neogene), but an increase in platform productivity linked to a decline in water depth and reduced exchange with the open ocean is one possibility (Panchuk et al., 2006). After rapid ice melting and re-flooding, ramp $\delta^{13}C$ declined, and distal

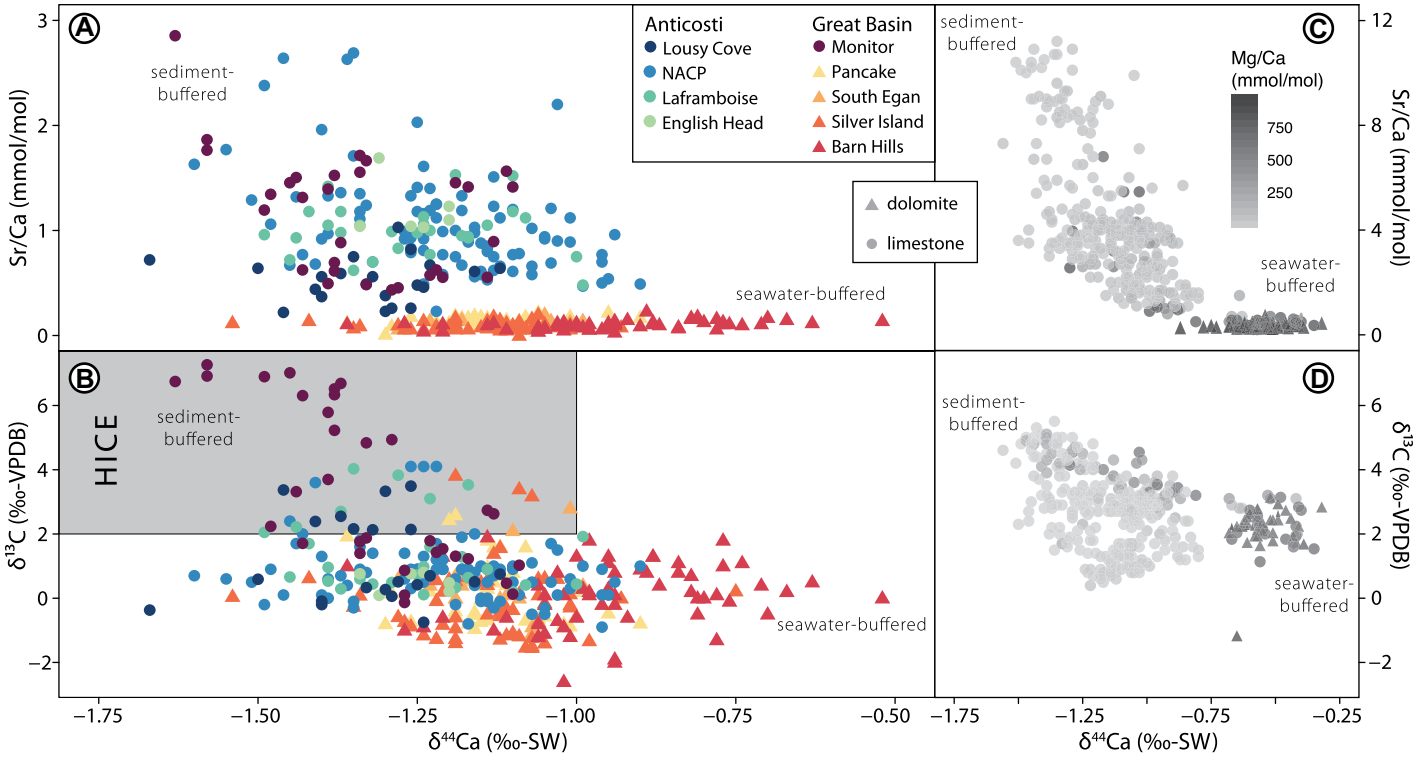

Figure 3. Cross-plots of geochemical data from the Late Ordovician interval of the Great Basin (Nevada and Utah, USA) and Anticosti Island (Canada), and comparison with a Neogene section from the Bahamas. (A) Sr/Ca versus $\delta^{44}Ca$ and (B) $\delta^{13}C$ versus. $\delta^{44}Ca$ for Ordovician samples. Great Basin samples are dolomitized at all locations except Monitor Range. SW—seawater, VPDB—Vienna Peedee belemnite; HICE—Hirnantian isotopic carbon excursion; NACP—New Associated Consolidated Paper drill core. (C) Sr/Ca versus $\delta^{44}Ca$ and (D) $\delta^{13}C$ versus $\delta^{44}Ca$ for Neogene Bahamas samples. Samples interpreted as "sediment buffered" largely retain a geochemistry of primary sediment and have low $\delta^{44}Ca$, high Sr/Ca, and high $\delta^{13}C$. Samples interpreted as "seawater buffered" record geochemistry of pore fluids buffered by seawater chemistry and have high $\delta^{44}Ca$, low Sr/Ca, and low $\delta^{13}C$. Note the change in vertical scale between Ordovician and Neogene Sr/Ca plots. Bahamas data are from Higgins et al. (2018) and Ahm et al. (2018).

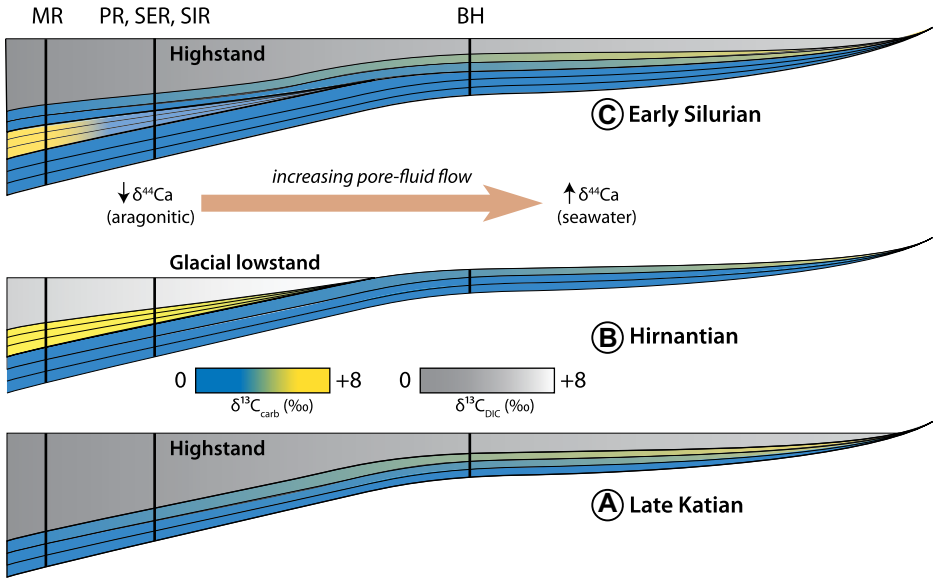

Figure 4. Conceptual model of geochemical development during Hirnantian sea-level fall and rise on a shallow-water carbonate platform. Aragonite is the primary carbonate mineral precipitate throughout. (A) Late Katian highstand scenario. (B) Hirnantian sea-level fall accompanied by a secular increase in platform (not necessarily open ocean) $\delta^{13}C$ result in deposition of shallow-water sediment with elevated $\delta^{13}C$ in distal settings. DIC—dissolved inorganic carbon; carb—carbonate. (C) During and following deglacial marine transgression, pore fluid is extensively flushed by seawater in nearshore settings, leading to seawater-buffered geochemistry. Low-magnitude fluid-flow rates in offshore settings allow sediment-buffered diagenesis, which largely retains the geochemistry of primary sediment. Note: $\delta^{13}C$ scale is based on the preserved record at Monitor Range, Nevada, USA. See Figure 2 for section abbreviations.

shallow-water deposits were buried by offshore highstand deposits (Fig. 4C).

Because pore-fluid circulation on carbonate platforms is most intense toward the basin margin (i.e., landward) and most sluggish in the basin center (i.e., offshore), the effects of early marine diagenesis were most pronounced in updip settings, where intense fluid flow caused fluid-buffered alteration (Fig. 4C) and, in the Great Basin, regional dolomitization. Those updip deposits acquired geochemical signatures reflecting the chemistry of seawater-like pore fluid ($\delta^{13}C$ and $\delta^{44}Ca$ both close to 0‰). In contrast, the synglacial aragonitic lowstand deposits were subjected to less advective flux and were more protected from this seawater-buffered alteration (at Monitor Range), generally retaining their primary geochemical signatures representing shallow-ramp environments, even after neomorphism to calcite (Fig. 4C).

Our analysis does not constrain the magnitude of the HICE for the global ocean and does not require that any component of the HICE represents changes in the partitioning of global carbon fluxes between carbonate and organic carbon (Kump and Arthur, 1999). Nevertheless, many deep basin sections record a small-magnitude HICE in organic carbon isotope ratios (Gorjan et al., 2012). Whereas these records

may themselves be sensitive to platform $\delta^{13}C$ (Oehlert and Swart, 2014), an ~1.5‰ global HICE has been suggested based on analysis of an open-ocean–facing section in Nevada (Ahm et al., 2017). Any such global signal would have been significantly modified in shallow carbonate settings by the processes considered here.

CONCLUSION

Paired analyses of $\delta^{44}Ca$ and Sr/Ca in ancient shallow-water carbonate sediments provide a novel framework with which to interpret carbon isotope excursions in the geologic record. This framework provides a way to identify primary versus diagenetic geochemical signals and to understand how early marine diagenesis varied in both space and time. Records of $\delta^{44}Ca$ and Sr/Ca of the HICE from the Great Basin and Anticosti Island are consistent with this framework; strata deposited in outboard settings prior to sea-level rise preserved the geochemistry of the primary sediment—sediment that reflects the chemical conditions (e.g., $\delta^{13}C$) on the local carbonate platform and not the global ocean (Swart, 2008). In contrast, strata deposited in shallow proximal settings during sea-level highs experienced early marine diagenesis under fluid-buffered conditions and recorded the geochemistry of these pore fluids (e.g., modified seawater). Many intervals of elevated $\delta^{13}C$ in the Paleozoic are characterized by spatially varying magnitudes, are short in duration, and are associated with sea-level changes (Farkaš et al., 2016). As such, the mechanisms invoked here for the Late Ordovician are likely to be widespread over Earth history, with broad implications for interpreting the environmental significance of $\delta^{13}C$ excursions and associated geochemical perturbations recorded in ancient platform carbonate rocks.

ACKNOWLEDGMENTS

Jones acknowledges the Donors of the American Chemical Society Petroleum Research Fund for partial support of this research. We are grateful to Ministère de l'Energie et des Ressources Naturelles du Québec for access to the NACP core. Ahm acknowledges support from the Simons Foundation (New York, SCOL 611878). Elizabeth Lundstom, Danielle Santiago Ramos, and Stephanie Moore provided laboratory support. We thank the three anonymous reviewers for constructive comments.

REFERENCES CITED

Ahm, A.-S.C., Bjerrum, C.J., and Hammarlund, E.U., 2017, Disentangling the record of diagenesis, local redox conditions, and global seawater chemistry during the latest Ordovician glaciation: Earth and Planetary Science Letters, v. 459, p. 145–156, https://doi.org/10.1016/j.epsl.2016.09.049.

Ahm, A.-S.C., Bjerrum, C.J., Blättler, C.L., Swart, P.K., and Higgins, J.A., 2018, Quantifying early marine diagenesis in shallow-water carbonate sediments: Geochimica et Cosmochimica Acta, v. 236, p. 140–159, https://doi.org/10.1016/j.gca.2018.02.042.

Baker, P.A., Gieskes, J.M., and Elderfield, H., 1982, Diagenesis of carbonates in deep-sea sediments; evidence from Sr/Ca ratios and interstitial dissolved Sr^{2+} data: Journal of Sedimentary Research, v. 52, p. 71–82.

Balthasar, U., and Cusack, M., 2015, Aragonite-calcite seas—Quantifying the gray area: Geology, v. 43, p. 99–102, https://doi.org/10.1130/G36293.1.

Banner, J.L., and Hanson, G.N., 1990, Calculation of simultaneous isotopic and trace element variations during water-rock interaction with applications to carbonate diagenesis: Geochimica et Cosmochimica Acta, v. 54, p. 3123–3137, https://doi.org/10.1016/0016-7037(90)90128-8.

Brand, U., and Veizer, J., 1980, Chemical diagenesis of a multicomponent carbonate system: 1. Trace elements: Journal of Sedimentary Petrology, v. 50, p. 1219–1236.

Brenchley, P.J., Marshall, J.D., Carden, G.A.F., Robertson, D., Long, D.G.F., Meidla, T., Hints, L., and Anderson, T.F., 1994, Bathymetric and isotopic evidence for a short-lived Late Ordovician glaciation in a greenhouse period: Geology, v. 22, p. 295–298, https://doi.org/10.1130/0091-7613(1994)022<0295:BAIEFA>2.3.CO;2.

Carpenter, R.M., Pandolfi, J.M., and Sheehan, P.M., 1986, The Late Ordovician and Silurian of the eastern Great Basin: Part 6. The Upper Ordovician carbonate ramp: Milwaukee Public Museum Contributions in Biology and Geology, v. 69, p. 1–48.

Caspard, E., Rudkiewicz, J.-L., Eberli, G.P., Brosse, E., and Renard, M., 2004, Massive dolomitization of a Messinian reef in the Great Bahama Bank: A numerical modelling evaluation of Kohout geothermal convection: Geofluids, v. 4, p. 40–60, https://doi.org/10.1111/j.1468-8123.2004.00071.x.

Desrochers, A., Farley, C., Achab, A., and Asselin, E., 2010, A far-field record of the end Ordovician glaciation: The Ellis Bay Formation, Anticosti Island, eastern Canada: Palaeogeography, Palaeoclimatology, Palaeoecology, v. 296, p. 248–263, https://doi.org/10.1016/j.palaeo.2010.02.017.

Fantle, M.S., and DePaolo, D.J., 2007, Ca isotopes in carbonate sediment and pore fluid from ODP Site 807A: The Ca^{2+}(aq)–calcite equilibrium fractionation factor and calcite recrystallization rates in Pleistocene sediments: Geochimica et Cosmochimica Acta, v. 71, p. 2524–2546, https://doi.org/10.1016/j.gca.2007.03.006.

Fantle, M.S., and Higgins, J., 2014, The effects of diagenesis and dolomitization on Ca and Mg isotopes in marine platform carbonates: Implications for the geochemical cycles of Ca and Mg: Geochimica et Cosmochimica Acta, v. 142, p. 458–481, https://doi.org/10.1016/j.gca.2014.07.025.

Farkaš, J., Frýda, J., and Holmden, C., 2016, Calcium isotope constraints on the marine carbon cycle and $CaCO_3$ deposition during the Late Silurian (Ludfordian) positive ^{13}C excursion: Earth and Planetary Science Letters, v. 451, p. 31–40, https://doi.org/10.1016/j.epsl.2016.06.038.

Finnegan, S., Bergmann, K., Eiler, J., Jones, D.S., Fike, D.A., Eisenman, I., Hughes, N., Tripati, A., and Fischer, W.W., 2011, The magnitude and duration of Late Ordovician–Early Silurian glaciation: Science, v. 331, p. 903–906, https://doi.org/10.1126/science.1200803.

Gorjan, P., Kaiho, K., Fike, D.A., and Xu, C., 2012, Carbon- and sulfur-isotope geochemistry of the Hirnantian (Late Ordovician) Wangjiawan (Riverside) section, South China: Global correlation and environmental event interpretation: Palaeogeography, Palaeoclimatology, Palaeoecology, v. 337–338, p. 14–22, https://doi.org/10.1016/j.palaeo.2012.03.021.

Gussone, N., Böhm, F., Eisenhauer, A., Dietzel, M., Heuser, A., Teichert, B.M.A., Reitner, J., Wörheide, G., and Dullo, W.-C., 2005, Calcium isotope fractionation in calcite and aragonite: Geochimica et Cosmochimica Acta, v. 69, p. 4485–4494, https://doi.org/10.1016/j.gca.2005.06.003.

Hardie, L.A., 1996, Secular variation in seawater chemistry: An explanation for the coupled secular variation in the mineralogies of marine limestones and potash evaporites over the past 600 my: Geology, v. 24, p. 279–283, https://doi.org/10.1130/0091-7613(1996)024<0279:SVISCA>2.3.CO;2.

Harris, M.T., and Sheehan, P.M., 1997, Carbonate sequences and fossil communities from the Upper Ordovician–Lower Silurian of the eastern Great Basin: Geology Studies, v. 42, p. 105–128.

Higgins, J.A., et al., 2018, Mineralogy, early marine diagenesis, and the chemistry of shallow-water carbonate sediments: Geochimica et Cosmochimica Acta, v. 220, p. 512–534, https://doi.org/10.1016/j.gca.2017.09.046.

Holmden, C., Panchuk, K., and Finney, S.C., 2012, Tightly coupled records of Ca and C isotope changes during the Hirnantian glaciation event in an epeiric sea setting: Geochimica et Cosmochimica Acta, v. 98, p. 94–106, https://doi.org/10.1016/j.gca.2012.09.017.

Hu, D., Zhang, X., Zhou, L., Finney, S.C., Liu, Y., Shen, D., Shen, M., Huang, W., and Shen, Y., 2017, Sr evidence from the epeiric Martin Ridge Basin for enhanced carbonate weathering during the Hirnantian: Scientific Reports, v. 7, p. 1–7, https://doi.org/10.1038/s41598-017-11619-w.

Jacobson, A.D., and Holmden, C., 2008, $\delta^{44}Ca$ evolution in a carbonate aquifer and its bearing on the equilibrium isotope fractionation factor for calcite: Earth and Planetary Science Letters, v. 270, p. 349–353, https://doi.org/10.1016/j.epsl.2008.03.039.

Jones, D.S., Fike, D.A., Finnegan, S., Fischer, W.W., Schrag, D.P., and McCay, D., 2011, Terminal Ordovician carbon isotope stratigraphy and glacioeustatic sea-level change across Anticosti Island (Québec, Canada): Geological Society of America Bulletin, v. 123, p. 1645–1664, https://doi.org/10.1130/B30323.1.

Jones, D.S., Creel, R.C., and Rios, B.A., 2016, Carbon isotope stratigraphy and correlation of depositional sequences in the Upper Ordovician Ely Springs Dolostone, eastern Great Basin, USA: Palaeogeography, Palaeoclimatology, Palaeoecology, v. 458, p. 85–101, https://doi.org/10.1016/j.palaeo.2016.01.036.

Kimmig, S.R., and Holmden, C., 2017, Multi-proxy geochemical evidence for primary aragonite precipitation in a tropical-shelf 'calcite sea' during the Hirnantian glaciation: Geochimica et Cosmochimica Acta, v. 206, p. 254–272, https://doi.org/10.1016/j.gca.2017.03.010.

Kump, L.R., and Arthur, M., 1999, Interpreting carbon-isotope excursions: Carbonates and organic matter: Chemical Geology, v. 161, p. 181–198, https://doi.org/10.1016/S0009-2541(99)00086-8.

Kump, L.R., Arthur, M.A., Patzkowsky, M., Gibbs, M., Pinkus, D.S., and Sheehan, P.M., 1999, A weathering hypothesis for glaciation at high atmospheric CO_2 during the Late Ordovician: Palaeogeography, Palaeoclimatology, Palaeoecology, v. 152, p. 173–187, https://doi.org/10.1016/S0031-0182(99)00046-2.

LaPorte, D.F., Holmden, C., Patterson, W.P., Loxton, J.D., Melchin, M.J., Mitchell, C.E., Finney, S.C., and Sheets, H.D., 2009, Local and global perspectives on carbon and nitrogen cycling during the Hirnantian glaciation: Palaeogeography, Palaeoclimatology, Palaeoecology, v. 276, p. 182–195, https://doi.org/10.1016/j.palaeo.2009.03.009.

McLaughlin, P.I., et al., 2016, Refining 2 km of Ordovician chronostratigraphy beneath

Anticosti Island utilizing integrated chemostratigraphy: Canadian Journal of Earth Sciences, v. 53, p. 865–874, https://doi.org/10.1139/cjes-2015-0242.

Melchin, M.J., and Holmden, C., 2006, Carbon isotope chemostratigraphy in Arctic Canada: Sea-level forcing of carbonate platform weathering and implications for Hirnantian global correlation: Palaeogeography, Palaeoclimatology, Palaeoecology, v. 234, p. 186–200, https://doi.org/10.1016/j.palaeo.2005.10.009.

Melchin, M.J., Mitchell, C.E., Holmden, C., and Storch, P., 2013, Environmental changes in the Late Ordovician–Early Silurian: Review and new insights from black shales and nitrogen isotopes: Geological Society of America Bulletin, v. 125, p. 1635–1670, https://doi.org/10.1130/B30812.1.

Oehlert, A.M., and Swart, P.K., 2014, Interpreting carbonate and organic carbon isotope covariance in the sedimentary record: Nature Communications, v. 5, p. 1–7, https://doi.org/10.1038/ncomms5672.

Panchuk, K., Holmden, C., and Leslie, S.A., 2006, Local controls on carbon cycling in the Ordovician midcontinent region of North America, with implications for carbon isotope secular curves: Journal of Sedimentary Research, v. 76, p. 200–211, https://doi.org/10.2110/jsr.2006.017.

Pogge von Strandmann, P.A.E., Desrochers, A., Murphy, M.J., Finlay, A.J., Selby, D., and Lenton, T.M., 2017, Global climate stabilisation by chemical weathering during the Hirnantian glaciation: Geochemical Perspectives Letters, v. 3, p. 230–237, https://doi.org/10.7185/geochemlet.1726.

Saltzman, M.R., and Thomas, E., 2012, Carbon isotope stratigraphy, *in* Gradstein, F.M., et al., eds., The Geologic Time Scale 2012: Amsterdam, Netherlands, Elsevier, p. 207–232, https://doi.org/10.1016/B978-0-444-59425-9.00011-1.

Saltzman, M.R., Young, S.A., Kump, L.R., Gill, B.C., Lyons, T.W., and Runnegar, B., 2011, Pulse of atmospheric oxygen during the late Cambrian: Proceedings of the National Academy of Sciences of the United States of America, v. 108, p. 3876–3881, https://doi.org/10.1073/pnas.1011836108.

Shao, Y., et al., 2018, Calcium and strontium isotope systematics in the lagoon-estuarine environments of South Australia: Implications for water source mixing, carbonate fluxes and fish migration: Geochimica et Cosmochimica Acta, v. 239, p. 90–108, https://doi.org/10.1016/j.gca.2018.07.036.

Swart, P.K., 2008, Global synchronous changes in the carbon isotopic composition of carbonate sediments unrelated to changes in the global carbon cycle: Proceedings of the National Academy of Sciences of the United States of America, v. 105, p. 13741–13745, https://doi.org/10.1073/pnas.0802841105.

Swart, P.K., and Eberli, G., 2005, The nature of the ^{13}C of periplatform sediments: Implications for stratigraphy and the global carbon cycle: Sedimentary Geology, v. 175, p. 115–129, https://doi.org/10.1016/j.sedgeo.2004.12.029.

Swart, P.K., and Melim, L., 2000, The origin of dolomites in Tertiary sediments from the margin of Great Bahama Bank: Journal of Sedimentary Research, v. 70, p. 738–748, https://doi.org/10.1306/2DC40934-0E47-11D7-8643000102C1865D.

Tang, J., Dietzel, M., Böhm, F., Köhler, S.J., and Eisenhauer, A., 2008, Sr^{2+}/Ca^{2+} and $^{44}Ca/^{40}Ca$ fractionation during inorganic calcite formation: II. Ca isotopes: Geochimica et Cosmochimica Acta, v. 72, p. 3733–3745, https://doi.org/10.1016/j.gca.2008.05.033.

Veizer, J., 1983, Trace elements and isotopes in sedimentary carbonates: Reviews in Mineralogy and Geochemistry, v. 11, p. 265–299.

Zhang, T., Shen, Y., Zhan, R., Shen, S., and Chen, X., 2009, Large perturbations of the carbon and sulfur cycle associated with the Late Ordovician mass extinction in South China: Geology, v. 37, p. 299–302, https://doi.org/10.1130/G25477A.1.

Printed in USA